# A label-free cardiac biomarker immunosensor based on phase-shifted microfiber Bragg grating

Tong Liu, Li-Li Liang, Peng Xiao, Li-Peng Sun, Yun-Yun Huang, Yang Ran, Long Jin, Bai-Ou Guan

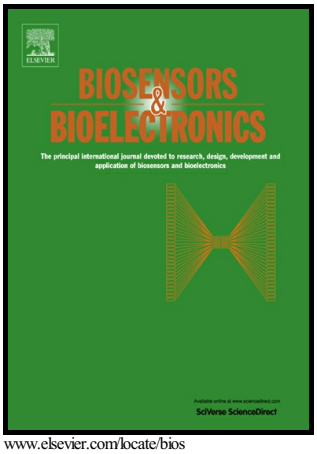


www.elsevier.com/locate/bios

PII: S0956-5663(17)30604-8
DOI: http://dx.doi.org/10.1016/j.bios.2017.08.061
Reference: BIOS9971

To appear in: *Biosensors and Bioelectronic*

Received date: 15 June 2017
Revised date: 18 August 2017
Accepted date: 30 August 2017

Cite this article as: Tong Liu, Li-Li Liang, Peng Xiao, Li-Peng Sun, Yun-Yun Huang, Yang Ran, Long Jin and Bai-Ou Guan, A label-free cardiac biomarker immunosensor based on phase-shifted microfiber Bragg grating, *Biosensors and Bioelectronic,* http://dx.doi.org/10.1016/j.bios.2017.08.061

# A label-free cardiac biomarker immunosensor based on phase-shifted microfiber Bragg grating

Tong Liu, Li-Li Liang, Peng Xiao, Li-Peng Sun, Yun-Yun Huang, Yang Ran*, Long Jin, Bai-Ou Guan

*Guangdong Provincial Key Laboratory of Optical Fiber Sensing and Communications, Institute of Photonics Technology, Jinan University, Guangzhou 510632, China*

***Abstract***—Fiber optics evanescent field based biosensor is an excellent candidate for label-free detection of cardiac biomarkers which is of great importance in rapid, early, and accurate diagnosis of acute myocardial infarction (AMI). In this paper, we report a compact and sensitive cardiac troponin I (cTn-I) immunosensor based on the phase-shifted microfiber Bragg grating probe which is functionalized. The fine reflective signal induced by the phase shift in modulation significantly improves the spectral resolution, enabling the ability of the sensor in perceiving an ultra-small refractive index change due to the specific capture of the cTn-I antigens. In buffer, a log-linear sensing range from 0.1 to 10 ng/mL and a limit of detection (LOD) of 0.03 ng/mL (predicted to be as low as 10.8 pg/mL) are obtained. Furthermore, with good specificity, the sensor can be applied in test of cTn-I in human serum samples. The proposed sensor presents superiorities such as improved integratability and portability, easy fabrication and operation, and intrinsic compatibility to the fiber-optic network, and thus has a promising prospect in "point-of-care" test for cardiac biomarkers and preclinical diagnosis.

***Keywords***—Optical microfibers; Phase-shifted Bragg gratings; fiber optical immunosensors; Cardiac troponin I; Acute myocardial infarction diagnosis



## 1. Introduction

Cardiovascular diseases (CVD) killed 17.5 million lives in 2012 and the number keeps growing, according to the newest report of the World Healthy Organizer (WHO, 2015). The acute myocardial infarction (AMI) or heart attack has been the one of the leading culprits of the mortality worldwide (Thygesen et al., 2012), which attributed to the blockage of the coronary arteries, triggering the scarcity of blood supply to the heart. AMI causes irreversible damage to the myocardial cells within a short time and probably brings out various complications, severely threatening the patient safety (White and Chew, 2008). Therefore, test of cardiac biomarkers which specifically reflect the damage of the heart muscle in patient's blood is of utmost importance depending on not only the capability of filling the absences in traditional diagnosis, such as the electrocardiograph (ECG) (Mahajan and Jarolim, 2011; Mohammed and Desmulliez, 2011), but also the potential of prognosticating the AMI at very early stage (Fathil, et al., 2015).

Labeling immunoassay techniques, including enzyme-linked immunosorbent assay (ELISA) and fluorescence immunoassay are frequently-used and powerful tools for detection of cardiac biomarkers with high sensitivity. However, the requirements of complicated and professional labeling process, large amount of the samples as well as reagents, and considerably long turn-around-time (TAT)(Tuteja et al., 2016; Fan et al., 2008) barricade the progress of those methods towards AMI diagnosis which needs simple and quick test results for making clinical decision as well as providing medical care to patients. As a consequence, label-free biosensors are developed recently to satisfy the yearning of rapid, accurate, and "point of care" (POC) test solutions for AMI diagnosis and early screening (King et al., 2016).

The label-free biosensors for detection of cardiac biomarkers mainly rely on the transducers which are generally categorized by mechanisms including optics (Wu et al., 2017; Diware et al., 2017; El-Said et al., 2016; Pawula et al., 2016; Zhang et al., 2014; Tang and Casas, 2014), electrics (Jo et al., 2017; Kim et al., 2016; Tuteja et al., 2016; Shin et al., 2016), magnetics (Meyer et al., 2007), and acoustics (Lee et al., 2011), presenting good performances and potentialities due to their simplicity in tests.

As an important optical method of detection which is fast developing and maturing, the fiber optics based biosensor becomes an eligible candidate for *in-situ* test of cardiac proteins by virtue of its distinguished advantages such as accepted cost, small and smart structure, high accuracy, biological compatibility, electromagnetic immunity, free of light coupling and telemeasurement (Wang and Wolfbeis, 2016). Based on the evanescent or plasma wave on the fiber surface, the immunoreactivity of cardiac biomarkers could be directly transduced by the resonant wavelength shift via the change of the surface refractive index (Luo et al., 2017; Sridevi et al., 2015; Masson et al., 2004).

*Corresponding author.
*E-mail address:* tranyang@jnu.edu.cn (Y. Ran)

Microfiber, which was defined as the fiber with a diameter below 10 micron, allowed the transmitting light to further interact with the surrounding medium because of the larger evanescent field (Ismaeel et al., 2013; Tong et al., 2003). Bragg grating written in

microfiber (mFBG) can further improve the competitiveness of the sensor because their superiorities are integrated, including purity of mode-coupling, relatively narrow bandwidth signal, and multiplexing capability (Guan et al., 2013). In addition, the nanoscale-period grating structure endows sensor with an intrinsically reflective signal. For this reason, mFBG can act as a micro-needle probe which is significant in the *in-vivo* bio-detection.

So far, the 193 nm excimer laser direct-writing technique has become a proven method of fabricating mFBG due to the high efficiency and versatility as well as low damage to the device (Xiao et al., 2016; Ran et al., 2015, 2012a, 2012b, 2011), effectively propelling the mFBG based sensor in detection of biomolecules, such as DNA (Cao et al., 2015; Sun et al., 2014) and cancer-indicated protein (Cao et al., 2017).

However, it's a huge challenge for proposing mFBG into AMI diagnosis because the critical concentration of cardiac biomarkers is extremely low. For example, cardiac troponin I (cTn-I), which is considered as a "golden standard" in AMI diagnosis (Fathil, et al., 2015; Mohammed and Desmulliez, 2011), has a critical concentration between 0.1-1 ng/mL in patient's blood. Even the concentration as low as 0.01 ng/mL is possibly related to chronicle heart failure and subclinical heart disease, etc. (Agewall et al., 2011). Such a concentration of molecules can hardly catch the awareness of the mFBG based biosensor which has relatively low outer refractive index (RI) sensitivity (several tens ~ a hundred nm/RIU) and broad signal bandwidth (larger than 1 nm).

Further reducing the fiber diameter to enhance the evanescent field seems like a plausible way for improving the sensitivity theoretically. However, for one thing, the nanoscaled period would be a big drag on the effective amplification of the RI response. For another and even more importantly, the insertion loss would inevitably be taken as a trade-off.

In this study, we demonstrated a novel label-free immunosensor for testing cTn-I antigen with high accuracy and specificity based on the phase-shifted microfiber Bragg grating (PS-mFBG). The π-phase-shift in modulation provided a narrow band notch signal to the reflective spectrum of the mFBG, greatly improving the resolution of the sensor. Combining the optimization of the fiber diameter, the PS-mFBG could effectively respond to a tiny RI change without sacrificing the signal quality, enabling the capability of detection of the variation caused by specific capture of ultra-small amount of cTn-I antigens in buffer conditions as well as in serum samples. The proposed cardiac biomarker sensor presents the improved portability and great convenience in fabrication, integration, and operation, holding its ticket for the entrance of POC test for AMI diagnosis at this stage and "the smart medical homes" in the future (Muse et al., 2017).

## 2. Material and methods

### *2.1 Materials*

Optical fiber was the telecom multimode silica fiber (62.5/125), which was purchased from Corning Inc. (USA). 98% sulfuric acid, hydrogen peroxide, hydrochloric acid, ethanol, phosphate buffered saline (PBS) and poly-L-lysine solutions (PLL) were from Sangon Biotech Co. Ltd. (China). Tris (hydroxymethyl) aminomethane (tris), β-mercaptoethanol, ethylenediaminetetraacetic acid (EDTA) and

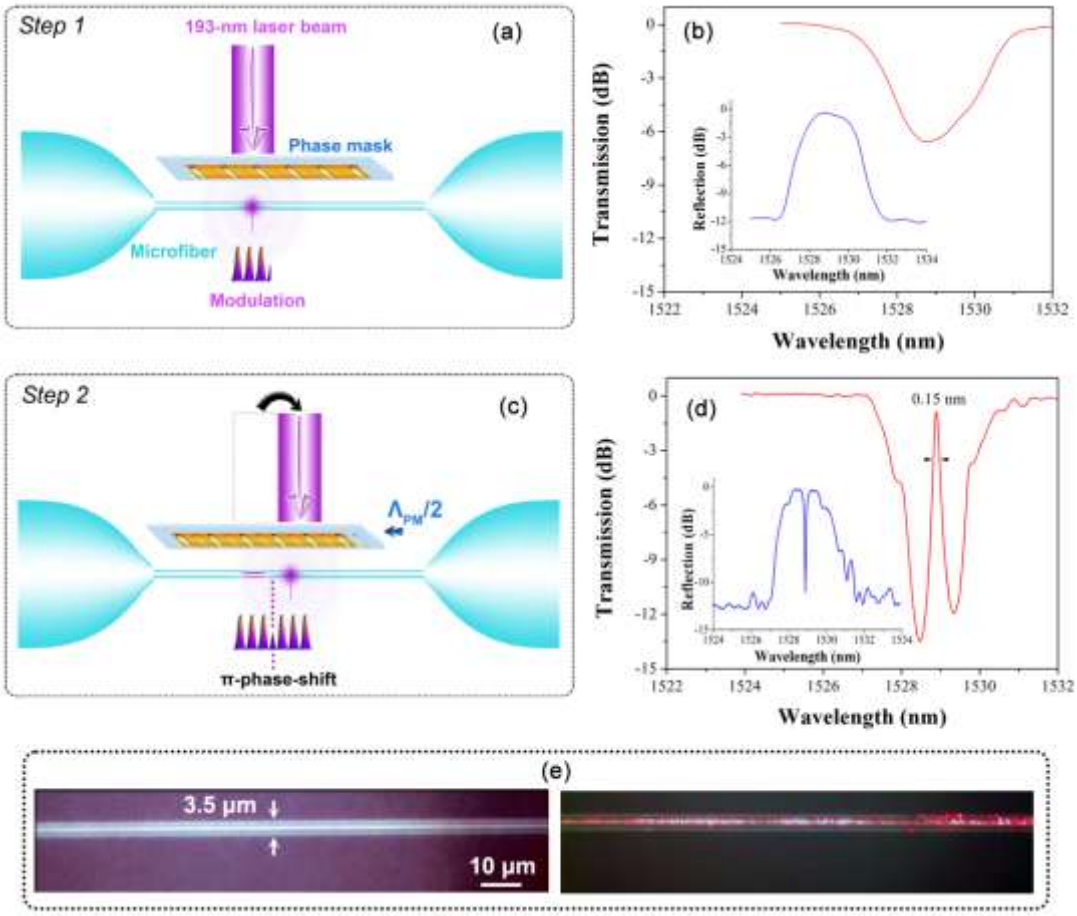


Fig. 1. Schematic of PS-mFBG fabrication. (a) The first step of the inscription; (b) Transmission and reflection spectra of the mFBG; (c) The second step of the inscription; (d) Transmission and reflection spectra of the PS-mFBG; (e)The microscopic image of the PS-mFBG: fiber profile (Left) and modulating structure (right).

urea were from AMRESCO LLC. (USA). Cardiac troponin protein (Recombinant human cardiac troponin I, cTn-I) and corresponding antibody including normal (Monoclonal mouse anti-cardiac troponin I, anti-cTn-I) and fluorescein isothiocyanate (FITC) -conjugated (Monoclonal mouse anti-cardiac troponin I, FITC-conjugated) were purchased from HyTest Ltd. (Finland). Human Albumin (ALB) and immunoglobulin G protein (IgG) were from Sino Biological Inc. (China). Human serum was from Biopanda Reagents Ltd. (UK). All the chemicals and biological materials were of analytical grade. Deionized (DI) water was used throughout the experiment.

### *2.2 Fabrication of the phase-shifted microfiber Bragg grating (PS-mFBG)*

The microfiber with a diameter of 3.5 μm was tapered by the flame-heated drawing technique (Ran et al., 2011). Here, the multimode fiber based microfiber provided a highly efficient FBG-inscription capability because it maintained a larger photosensitive region (Ran et al., 2012b). The diameter of the microfiber was optimized by considering both the evanescent field and insertion loss (Fig. S1 and S2). A 193 nm excimer laser (BraggStar Industrial, Coherent, Inc.,) was used to conduct the intracore refractive index change on the microfiber. The repetition rate of the laser was maintained to 200 Hz. An aperture slot was used to strictly shape the profile of the incident beam to a perfect rectangle with 6 mm ×1.5 mm (Height × Width). The UV energy density was adjusted to 100 mJ/cm$^2$ per pulse. A uniform phase mask (Ibsen, Ltd.,) with a pitch of 1072.15 nm was chosen. A broadband source with a wavelength range of 1250–1650 nm and an average power density of -30 dBm/nm was used to provide a reference transmission. A high-resolution optical spectrum analyzer (BOSA-lite, Argon Photonics Labs. S. L.U.,) with a limit-resolution of 0.2 pm was used to monitor the spectra of the grating. A home-made controlling system was implemented to drive the excimer laser beam as well as the phase mask (Fig. S3). Fig. 1 showed the PS-mFBG inscription method, which included two steps.

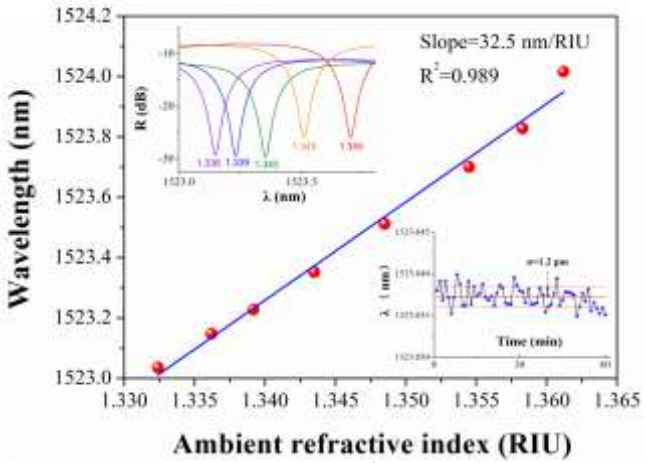


Fig. 2. Sensitivity of the PS-mFBG for ambient refractive index (RI). Inset (upper left): the reflective spectrum (notch) of PS-mFBG varied with the change of ambient RI. Inset (lower right): the long-time wavelength stability of the notch when the PS-mFBG was immersed into the DI water. "*R*", "*R2*", "*σ*" and "*λ*" represented the reflectivity, regression factor, standard deviation and wavelength, respectively.

Firstly, through the fix-positional exposure with 3 minutes, a conventional type-I grating was inscribed into the microfiber with a reflectivity of 7 dB, according to Fig. 1(a) and 1(b).

Secondly, driven by a PI step-motor along the axial direction, the laser beam moved a distance across an entire beam width of 1.5 mm, aiming at a new position closely to the original inscribed position. Meanwhile, the phase mask was given a displacement of a half pitch (~536 nm) by a nanoscale-precision translation stage for introducing a π-phase-shift into the refractive index modulation on the fiber core. Through another 3 minutes fix- positional exposure, a PS-mFBG was done with strength of 13.5 dB. The total length of the PS-mFBG was 3 mm. Therefore, the effective volume of the optical sensor was smaller than 3 ×10$^{-5}$ mm$^3$. A notch with a bandwidth of 150 pm was observed in the middle of the grating spectrum, denoting that the π-phase-shift was successfully created among the intracore modulation, as shown in Fig. 1(c) and 1(d). The Q-factor of the notch was ~1.01 ×10$^4$.

The microscopic image described the profile of the PS-mFBG in Fig. 1(e) left. Moreover, through guiding a red-laser into the microfiber, the nano-scale modulating structure could be observed at the PS-mFBG region via the diffraction, as show in Fig. 1(e) right.

### *2.3 Refractive index detection of the PS-mFBG*

Given that the ambient refractive index (RI) sensitivity of the fiber-optical evanescence based sensors was the paramount prerequisite for the label-free measurement of the biomolecules, the response of the PS-mFBG in solution with different RI was tested by tracing the notch in the reflection spectrum. The liquid that we used was the mixture of the ethanol and the DI water. The RI of the liquid could be deployed by changing the concentration of the ethanol. The range of variation was from 1.333 to 1.365. The temperature was controlled to 23 $^0$C. According to Fig. 2, the wavelength of the notch changed with increase of the RI, building up a mapping of $\Delta\lambda \rightarrow \Delta RI$. Here, the sensor with a wavelength encoding method could eliminate the impact of the variation of the intensity baseline which was caused by the absorption of hydroxyl ion ($OH^-$) in the fiber. The responding curve presented good linearity with sensitivity of ~32.57 nm/RIU with a relative standard deviation of 0.0215 which was measured through three trials (Fig. S4). In the following, maintaining the PS-mFBG in DI water, the long-time wavelength jitter of the notch was tested in order to provide the resolution of the sensing signal under liquid environment. According to the standard deviation of the wavelength distribution, it could be deduced that the resolution of the PS-mFBG was 1.2 pm. Therefore, the proposed sensor presented a limit of detection (LOD) to as low as 3.7×10$^{-5}$ RIU. Considering that the response of the mFBG normally presented a quadratic tendency in a large dynamic RI range, the sensor could be more sensitive under condition of high RI. Through calculation, the RI sensitivity was estimated to 67 nm/RIU at the RI=1.40 (Fig. S5). Accordingly, the LOD of the sensor could reach 1.8×10$^{-5}$ RIU, manifesting its capability of the sensor in transducing an ultra-small variation of outer RI to a distinguishable signal change.

### *2.4 Functionalization for the cTn-I immunosensor*

In order to achieve specificity of detection, functionalization for effectively discriminating the cTn-I antigen was indispensable to the sensor. Here, we chose layer-by-layer self-assembly technique to achieve functionalization of sensor with simplicity and high efficiency

(Whitesides and Grzybowski, 2002; Bertrand et al, 2000). The functionalization of the PS-mFBG probe followed the procedures below, as shown in Fig. 3(a). Note that at the end of each procedure, the DI water was used to rinse the probe for 5 min to remove the residuals.

1) Hydroxylation to the silica surface. The PS-mFBG probe was treated with the piranha solution prepared by mixing the 98% sulfuric acid and 30% hydrogen peroxide with volume ratio of 3:1 for 30 minutes.

2) Decoration of linked layer of PLL. The probe was immersed into the PLL solution (0.1% w/v, molecular weight: 150 to 300 kg/mol) for 1 hour.

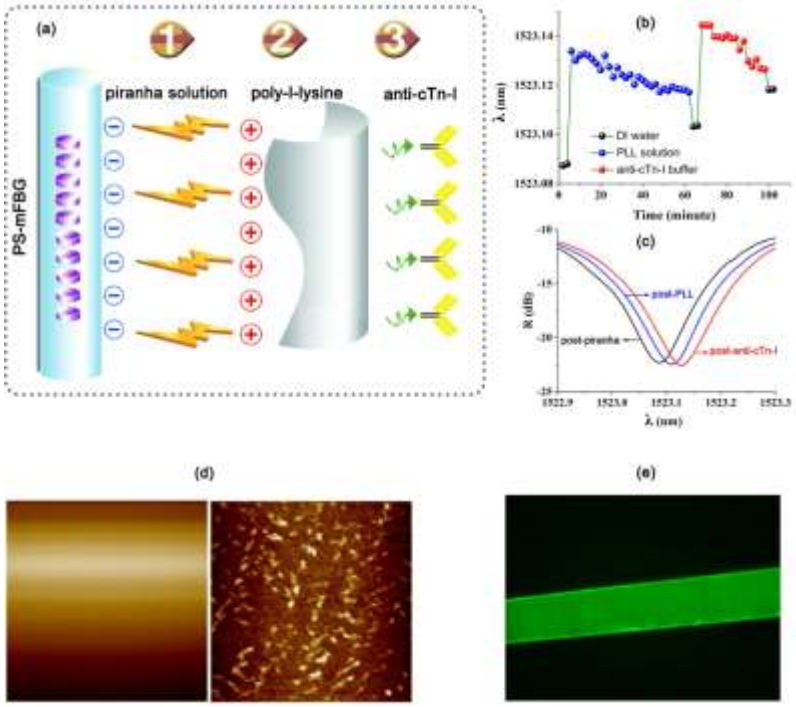


Fig. 3. (a) Schematic of the functionalized process for detection of cTn-I; (b) Wavelength variation of the notch signal throughout the functionalized process; (c) Spectrum of the notch recorded at the end of the each step in DI water; (d) Comparison of the AFM images between the surface of the bare fiber (left) and functionalized fiber anchored with anti-cTn-I (right); (e) image from fluorescence microscope of the fiber which immobilized the labeled anti-cTn-I.

3) Implementation of the immunological recognition. The probe was immersed into the anti-cTn-I solution (10 μg/mL) for 30 min. The solution was prepared through diluting the anti-cTn-I into the PBS with a pH of 7.4. Providing just one cycle of treatment, the sensor tip was successfully functionalized with a monolayer of anti-cTn-I (Decher et al., 1992).

Fig. 3(b) recorded the spectral response of the notch throughout the whole functionalization. Regarding that the wavelength of the notch presented little difference in the piranha solution and DI water because there was no change of surface feature of the probe, the response was just recorded from the DI water after the hydroxylation procedure.

By transferring the probe to the PLL solution, the wavelength signal showed an abrupt red-shift of ~50 pm at beginning but then experienced a slow blue-shift during the following time. At the end, after rinsing the probe through the DI water, an obvious decrease occurred to the notch's wavelength, inferring the free residuals of PLL molecules were removed. As well, the third procedure of immuno-functionalization exhibited a similar evolution of the signal. The reason of the wavelength evolutions of those two procedures probably attributed to the electrostatic adsorption which excessively assembled the materials at first, leading to a large increase of surface refractive index. Yet the surface refractive index reduced gradually in the following period owing to the re-dissolving of the redundant materials. Depending on the spectral wavelength recorded at the end of each procedure in the DI water, as shown in Fig. 3(c), it could be inferred that the corresponding materials were effectively anchored onto the probe surface.

In order to approve the functionalization, two kinds of representation methods, the atomic force microscopy (AFM) and fluorescent microscopy, were employed.

Fig. 3(d) illustrated the contrast of the surface feature between the probes without and with functionalized layer anchored with anti-cTn-I by use of the AFM. The functionalized fiber was measured after a 24-h drying process. It could be seen that the functionalized probe had a more wrinkled surface than the bare one, implying that the bio-materials were adhered onto the silica surface. Further, a kind of cTn-I antibody conjugated with FITC was applied to verify the functionalization via the fluorophores. The preparation of the solution of labeled anti-cTn-I was as the same as that of unlabeled anti-cTn-I. As shown in the fluorescence-microscopic image at in Fig. 3(e), the profile of the fiber was clearly observed through the green fluorescence which was stimulated by 455 nm laser integrated in the fluorescent microscopy. Thus, it could be confirmed that the specific recognition layer was successfully assembled onto the sensing probe. And the tests of the sensor with long-time storage also showed that the functional layer had a good long-term stability (Fig. S10).

## 3. Results and discussion

The experimental setup for detection of cTn-I antigen was illustrated in Fig. S6.

### *3.1 Sensitivity and detection limit*

The cTn-I antigen was reconstituted by the Tris-urea buffer which includes 20 mM Tris- HCl (pH 7.4), 7 M urea, 5 mM EDTA, and 15 mM β-meryrcaptoethanol with different concentrations. At first, a typically critical concentration of 0.3 ng/mL was chosen. The probe

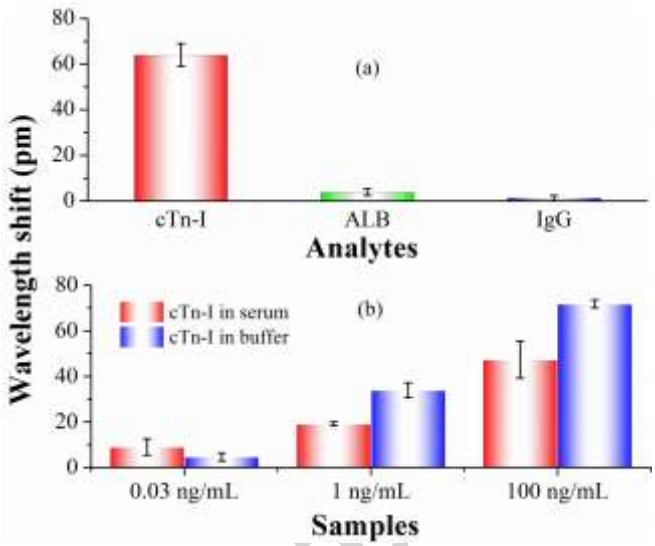


Fig. 5. (a) Measured responses to the antigens of specificity (cTn-I) and non-specificity (ALB and IgG) with the same bulk concentration of 10 ng/mL. (b) Detection of cTn-I in human serum and in buffer.

was surrounded by the cTn-I solution which was drawn through the injector. According to Fig. S7(a), the wavelength of the notch evolved with time, denoting that the kinetically immune binding was ongoing. Here, owing to the higher RI of ~1.40 attributed to the tris-urea buffer (Table S1), the signal appeared at a longer wavelength of 1525.226 nm from the start point of the binding process. The response rate was rapid at first half-hour and smooth at another. By comparing the spectrum of the started and completed points, the corresponding Δλ was read out to be ~18 pm.

In the following, a series of cTn-I solution with different concentrations were used for tests, as shown in Fig. S7(b). Note that, in order to reuse the fiber sensing element for eliminating the variations of using different ones, the used probe needed to be rinsed by piranha solution to restore after each test and then process the functionalization once again. It could be observed that the recorded Δλ of the notch increased in accordance with the elevation of the target concentration. Referring the optical response in the buffer without cTn-I antigen (0 ng/mL), the actual spectrum resolution of the probe was 1.28 pm which was slightly higher than bare PS-mFBG sensor probably due to the functionalization layer as well as the higher RI solution.

Through the repeatability tests at each concentration (C), the detecting curve could be drawn with error bars which represented the standard deviation of three independent measurements with the same probe, as shown in Fig. 4. In general, the curve exhibited an "*S*" shape with the range of 0.03 to 100 ng/mL. The lowest concentration of cTn-I antigen (0.03 ng/mL) in the experiment could be transduced by a Δλ of 4.7±1.7 pm of the sensor. The response curve could be fitted by Logistic function (Liu et al., 2017a, 2017b, 2015) as:

$$\Delta\lambda = 75.1075 - \frac{76.2165}{(1+C/1.32094)^{0.71442}}, \quad (R^2 = 0.9964) \qquad (1)$$

As a result, regarding the spectrum resolution of 1.28 pm, the LOD of the proposed sensor was estimated to as low as 10.8 pg/mL, showing a significant improvement compared with previously reported label-free fiber-optic cardiac biomarker sensors with LOD at the scale of ng/mL (Luo et al., 2017; Sridevi et al., 2015; Masson et al., 2004) and fulfilling the requirement of early AMI diagnosis (Fathil, et al., 2015). Moreover, further improving LOD is available by use of a PS-mFBG with a narrower notch signal which can be obtained simply by enhancing the reflectivity of the grating (Fig. S8).

From the detecting curve, a log-linear responding section was found with the range from 0.1 to 10 ng/mL. The relationship could be represented as Δλ=26.37× log(C)+34.54, ($R^2$=0.9987).

In order to evaluating the detecting capability of the probe in a shorter time, the responses in 30 min and 15 min were drawn, respectively, shown in Fig. S9. In the linear range, the curves exhibited smaller slopes compared with the 1-h curve, because the immunologic process was not entirely finished. There were certain trade-offs of the sensitivity, although, the sensor was still available within shorter turn-around-time, which would benefit the rapid screening for high risk patients. Furthermore, the overall test period is supposed to shorten by optimization of the environmental control, including pH of solution as well as temperature (Masson et al., 2004).

### *3.2 Specificity*

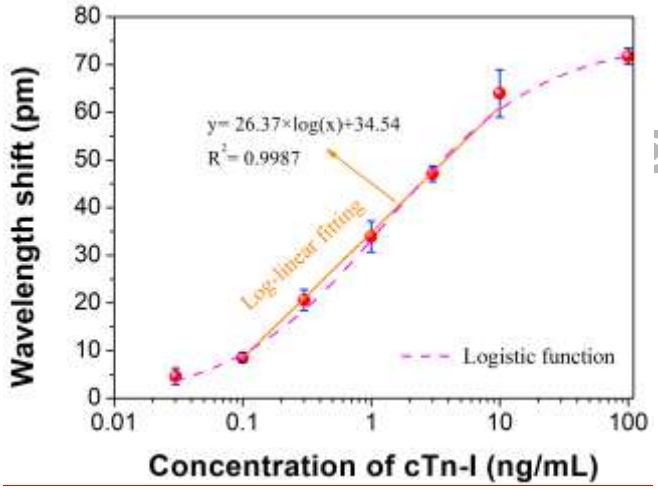


Fig. 4. 1-h Optical responses to cTn-I spiked in buffer.

Finally, two kinds of non-specific proteins -ALB and IgG, which widely existed in human plasma, were adopted to demonstrate the specificity of the probe (Jo et al., 2017; Wang et al., 2015; Vashist et al., 2015). The antigens were diluted in the PBS with the same concentration of 10 ng/mL, in accordance with the maximum cTn-I concentration in log-linear responding section. From the 1-hour test result illustrated in Fig. 5 (a), the mean $\Delta\lambda s$ were only 3.8 pm and 1.23 pm corresponding to the ALB and IgG, respectively. Therefore, the proposed sensor responded lower by more than an order of magnitude for both non-specific proteins, revealing its high specificity.

The cTn-I detection in human serum was then explored. The different amount of cTn-I antigens were directly put into the human serum samples without any pretreatment for demonstrating the detection under a more complex and realistic environment. As shown in Fig. 5(b), it could be inferred that the binding of non-specific biomolecules in serum was slightly enhanced, according to that the optical response in serum sample was higher than that in buffer sample at the critical cTn-I concentration (0.03 ng/mL). Despite this, the specific responses dominated the cTn-I detection in serum samples with higher concentrations. The lower responses compared with buffer samples were probably due to that the serum was neither the optimal environment for activating the cTn-I antigens nor at the optimized RI sensitive region of the PS-mFBG (Fig. S5 and Table S1). The result showed that the PS-mFBG based cTn-I sensor could also serve the detection in serum environment, which is essential in POC testing applications.

## 4. Conclusion

A sensitive label-free fiber-optic based immunosensor for quantitative cTn-I testing has been proposed by using a phase-shifted Bragg grating directly inscribed in microfiber. The fine notch signal in the grating spectrum greatly enhances the ability of the sensor in detecting an extremely small amount of immune binding events, which is essential for AMI diagnosis at very early stage. A cTn-I concentration of 10.8 pg/mL is enough to arouse the response of the sensor with high specificity, much lower than those of the previously reported label-free fiber optic cardiac marker sensors. According to the log-linear range of the concentration between 0.1~10 ng/mL, measurements with shorter detection time are analyzed to demonstrate the potential of the sensor in the fast screen of the high risk patients. The cTn-I sensor could also serve in human serum samples. The 193 nm laser inscription technique also allows the further improvement of LOD by increasing reflectivity of the grating to provide the optical signal with higher finesse and thus the higher spectral resolution. The proposed sensing probe is compact and feasible, easy to handle, fabricate and network, making itself a competitive candidate in POC diagnosis of AMI.

## Acknowledgement

We thank Dr. C. Huang of Guangdong General Hospital for the helpful suggestions. This work was supported by National Natural Science Foundation of China (Grant No. 61775082 and 61405074), Guangdong Natural Science Foundation (Grant No. 2015A030313324), Pearl River S&T Nova Program of Guangzhou (Grant No. 201610010151) and the Fundamental Research Funds for the Central Universities.

## Appendix A. Supplementary data

Supplementary data associated with this article can be found in the online version at XXXX

## References

Agewall, S., Giannitsis,E., Jernberg,T., Katus,H., 2011.Eur. Heart J. 32,404–411.
Bertrand, P., Jonas, A., Laschewsky, A., Legras, R., 2000. Macromol. Rapid Commun. 21, 319–348.
Cao, Y., Guo, T., Wang, X., Sun, D., Ran, Y., Feng, X., Guan, B.O, 2015. Opt. Express 23, 27061–27070.
Cao, Y., Wang, X.D., Guo, T., Ran, Y., Feng, X.H., Guan, B.O., Yao, J.P., 2017. Sensors Actuat.B-Chem. 245, 583–589.
Decher, G., Hong, J.D., Schmitt, J., 1992. Thin Solid Films 210, 831–835.
Diware, M.S., Cho, H.M., Chegal, W., Cho, Y.J., Kim, D.S., O, S.W., Kim, K.-S., Paek, S.-H., 2017. Biosens. Bioelectron. 87, 242–248.
El-Said, W.A., Fouad, D.M., El-Safty, S.A., 2016. Sensors Actuat.B-Chem. 228, 401–409.
Fan, X., White, I.M., Shopova, S.I., Zhu, H., Suter, J.D., Sun, Y., 2008. Anal. Chim. Acta 620, 8–26.

Fathil, M.F.M., Md Arshad, M.K., Gopinath, S.C.B., Hashim, U., Adzhri, R., Ayub, R.M., Ruslinda, A.R., Nuzaihan M.N., M., Azman, A.H., Zaki, M., Tang, T.H., 2015. Biosens. Bioelectron. 70, 209–220.
Guan, B.O., Li, J., Jin, L., Ran, Y., 2013. Opt. Fiber Technol. 19, 793–801.
Ismaeel, R., Lee, T., Ding, M., Belal, M., Brambilla, G., 2013. Laser Photon. Rev. 7, 350–384.
Jo, H., Her, J., Lee, H., Shim, Y.B., Ban, C., 2017. Talanta 165, 442–448.
Kim, K., Park, C., Kwon, D., Kim, D., Meyyappan, M., Jeon, S., Lee, J.-S., 2016. Biosens. Bioelectron. 77, 695–701.
King, K.R., Grazette, L.P., Paltoo, D.N., McDevitt, J.T., Sia, S.K., Barrett, P.M., Apple, F.S., Gurbel, P.A., Weissleder, R., Leeds, H., Iturriaga, E.J., Rao, A.K., Adhikari, B., Desvigne-Nickens, P., Galis, Z.S., Libby, P., 2016. JACC Basic to Transl. Sci. 1, 73–86.
Lee, J., Choi, Y.S., Lee, Y., Lee, H.J., Lee, J.N., Kim, S.K., Han, K.Y., Cho, E.C., Park, J.C., Lee, S.S., 2011. Anal. Chem. 83, 8629–8635.
Liang, G., Luo, Z., Liu, K., Wang, Y., Dai, J., Duan, Y., 2016. Crit. Rev. Anal. Chem. 46, 213–223.
Liu, L., Zhou, X., Lu, Y., Shan, D., Xu, B., He, M., Shi, H., Qian, Y., 2017a. Biosens. Bioelectron. 97, 16–20.
Liu, L., Zhou, X., Wilkinson, J.S., Hua, P., Song, B., Shi, H., 2017b. Sci. Rep. 7, 3655.
Liu, L., Zhou, X., Shi, H., 2015. Biosens. Bioelectron. 72, 300–305.
Luo, B., Wu, S., Zhang, Z., Zou, W., Shi, S., Zhao, M., Zhong, N., Liu, Y., Zou, X., Wang, L., Chai, W., Hu, C., Zhang, L., 2017. Opt. Express 8, 57–67.
Mahajan, V.S., Jarolim, P., 2011. Circulation 124, 2350–2354.
Masson, J. F., Obando, L., Beaudoin, S., Booksh, K., 2004. Talanta 62, 865–870.
Meyer, M.H.F., Hartmann, M., Krause, H.J., Blankenstein, G., Mueller-Chorus, B., Oster, J., Miethe, P., Keusgen, M., 2007. Biosens. Bioelectron. 22, 973–979.
Mohammed, M.I., Desmulliez, M.P.Y., 2011. Lab Chip 11, 569–595.
Muse, E.D., Barrett, P.M., Steinhubl, S.R., Topol, E.J., 2017. Lancet 389, 358.
Pawula, M., Altintas, Z., Tothill, I.E., 2016. Talanta 146, 823–830.
Ran, Y., Jin, L., Gao, S., Sun, L.P., Huang, Y.Y., Li, J., Guan, B.O., 2015. Opt. Lett. 40, 3802–3805.
Ran, Y., Jin, L., Sun, L.P., Li, J., Guan, B.O., 2012a. Opt. Lett. 37, 2649–2651.
Ran, Y., Jin, L., Tan, Y.N., Sun, L.P., Li, J., Guan, B.O., 2012b. IEEE Photonics J. 4, 181–186.
Ran, Y., Tan, Y.N., Sun, L.P., Gao, S., Li, J., Jin, L., Guan, B.O., 2011. Opt. Express 19, 18577–18583.
Shin, S.R., Zhang, Y.S., Kim, D.-J., Manbohi, A., Avci, H., Silvestri, A., Aleman, J., Hu, N., Kilic, T., Keung, W., Righi, M., Assawes, P., Alhadrami, H.A., Li, R.A., Dokmeci, M.R., Khademhosseini, A., 2016. Anal. Chem. 88, 10019–10027.
Sridevi, S., Vasu, K.S., Asokan, S., Sood, A.K., 2015. Biosens. Bioelectron. 65, 251–256.
Sun, D., Guo, T., Ran, Y., Huang, Y., Guan, B.O., 2014. Biosens. Bioelectron. 61, 541–546.
Tang, L., Casas, J., 2014. Biosens. Bioelectron. 61, 70–75.
Thygesen, K., Alpert, J.S., White, H.D., Jaffe, A.S., Katus, H.A., Apple, F.S., Lindahl, B., Morrow, D.A., Chaitman, B.R., Clemmensen, P.M., Johanson, P., Hod, H., Underwood, R., Bax, J.J., Bonow, R.O., Pinto, F., Gibbons, R.J., Fox, K.A., Atar, D., Newby, L.K., Galvani, M., Hamm, C.W., Uretsky, B.F., Steg, P.G., Wijns, W., Bassand, J.-P., Menasche, P., Ravkilde, J., Ohman, E.M., Antman, E.M., Wallentin, L.C., Armstrong, P.W., Simoons, M.L., Januzzi, J.L., Nieminen, M.S., Gheorghiade, M., Filippatos, G., Luepker, R. V, Fortmann, S.P., Rosamond, W.D., Levy, D., Wood, D., Smith, S.C., Hu, D., Lopez-Sendon, J.-L., Robertson, R.M., Weaver, D., Tendera, M., Bove, A.A., Parkhomenko, A.N., Vasilieva, E.J., Mendis, S., 2012. J. Am. Coll. Cardiol. 60, 1581–1598.
Tong, L., Gattass, R.R., Ashcom, J.B., He, S., Lou, J., Shen, M., Maxwell, I., Mazur, E., 2003. Nature 426, 816–819.
Tuteja, S.K., Chen, R., Kukkar, M., Song, C.K., Mutreja, R., Singh, S., Paul, A.K., Lee, H., Kim, K.-H., Deep, A., Suri, C.R., 2016. Biosens. Bioelectron. 86, 548–556.
Vashist, S.K., Schneider, E.M., Zengerle, R., Von Stetten, F., Luong, J.H.T., 2015. Biosens. Bioelectron. 66, 169–176.
Wang, X., Wolfbeis, O.S., 2016. Anal. Chem. 88, 203–227.
Wang, Q., Liu, F., Yang, X., Wang, K., Wang, H., Deng, X., 2015. Biosens. Bioelectron. 64, 161–164.
White, H.D., Chew, D.P., 2008. Lancet 372, 570–584.
Whitesides, G.M., Grzybowski, B., 2002. Science 295, 2418 -2421.
WHO, 2015.Cardiovascular diseases. World Health Organization. <http://www.who. int/mediacentre/factsheets/fs317/en/>



Table of Contents

## Highlights

1、 Phase-shifted microfiber Bragg grating sensor is applied in label-free detection of cardiac biomarkers.

2、 The detection limit for cTn-I of the proposed sensor reaches the scale of **pg/mL** (10.8 pg/mL).

3、 The proposed sensor can serve the test of cTn-I in human serum samples.